

# The performance of a finite impedance wedge barrier

D. Ouis<sup>a)</sup>

(Received 2002 September 17; revised 2003 September 24; accepted 2003 October 02)

The problem of sound screening by a wedge shaped barrier with general boundary conditions is considered. The theoretical methods used for evaluating the effectiveness of a noise barrier on the ground often appeal to one model for considering the wave reflection from the ground, and another model accounting for the wave diffraction at the top of the wedge barrier. For a point-like sound source, there are several attractive models for evaluating the sound field diffracted by either an ideally hard or an ideally soft wedge, but few treat the case of a wedge of more general surface boundary conditions. The purpose of the present work is to carry out a numerical investigation based on an existing diffraction model where the edge diffracted field is given as a high frequency asymptotic expression. The sound excitation source is taken as linear and parallel to the edge of the wedge, hence the two-dimensional character of the problem. The expression of the field diffracted by the edge of the absorbing wedge is adapted from a model where it is developed from the solution for plane wave incidence. More specifically, the solution to the case of the line source in that model is elaborated by considering a wave spectrum decomposition of a cylindrical wave. Numerical results of calculations on an absorbing wedge in free space show that the amplitude of the edge diffracted field increases with increasing hardness of the wedge. This field amplitude is also found to increase with an increasing value of the opening angle of the wedge, which is in agreement with the results for the case of an ideally hard wedge irradiated by a spherical source. Another point of interest, which is also considered in this study, is the case of a hard wedge on a ground with mixed boundary conditions, and which is considered for both the case of a point source and the case of a line source. Further examples are considered for predicting the insertion loss of an absorbing barrier in a typical road traffic situation. The barrier is erected on ground consisting of a combination of two grounds with different impedances, namely that of asphalt on the source side, and of grass on the receiver side. The results of numerical calculations show that the noise shielding performance of the impedance barrier diminishes both for increasing hardness of the barrier and for increasing value of the barrier angle. This latter conclusion is also in agreement with previous findings for a hard wedged barrier, with a point-like sound source. The divergence of the sound source is also found to have a minor effect on evaluating the effectiveness of the noise barrier. © 2003 Institute of Noise Control Engineering.

Primary subject classification: 31.1; Secondary subject classification: 76.1.1

## 1. INTRODUCTION

Noise emanating from road traffic is often considered a serious problem for people dwelling near roads. Artificial barriers or elevated road side banks are thus often used in residential areas for reducing this kind of noise. However, researchers are often in need of theoretical prediction schemes for foreseeing the performance of newly designed noise barriers before running full-scale tests on prototypes. Theoretical predictions may be made either by numerical techniques, or by means of analytical models. In this latter case, the most widespread techniques require the combination of a model accounting for the reflection of sound waves on the ground, and another model for treating the diffraction of waves by a straight-edged barrier. During the past few decades there has been intensive research activity in this field, and as a consequence several accurate models have been developed.

For more than a century the problem of wave scattering by a wedge has been a subject of increasing interest and continuous development. Exact analytical solutions have first been formulated for the case of plane wave incidence,

and then generalized to the cases of cylindrical and spherical wave incidence. Cases where the wave source is point-like or with the wedge faces not perfectly hard or perfectly soft but of more general boundary conditions are significantly more difficult, and they often necessitate special techniques for their solution. In this respect an ideal straight traffic line is often represented, with a satisfactory degree of approximation by an incoherent linear sound source with the main acoustical characteristic being that the pressure field amplitude variation exhibits a space variation inversely proportional to the distance  $r$  from the sound source. However, and in the absence of more suitable models, the present paper considers the case of a sound pressure field variation following a  $1/\sqrt{r}$  function, typical for a coherent source.

In acoustics, the problem of the wedge with finite impedance faces has been the subject of research for some years,<sup>1-6</sup> as well as for different applications regarding the case of a hard wedge.<sup>7,8</sup> Although some special attention has been devoted to particular applications of acoustical scattering by wedges,<sup>9-12</sup> it may be said that most of the research on this topic has been conducted for various applications in electromagnetism.<sup>13-18</sup>

<sup>a)</sup> Malmö University, School of Technology and Society, S-205 06 Malmö, Sweden; E-mail [djamel.ouis@ts.mah.se](mailto:djamel.ouis@ts.mah.se).

## 2. DIFFRACTION OF A CYLINDRICAL WAVE BY AN IMPEDANCE WEDGE

The problem of diffraction by an impedance wedge has been solved exactly by Maliuzhinets for a plane incident wave,<sup>1</sup> and the solution for a line source was made by considering the plane wave spectrum decomposition of a cylindrical wave.<sup>16</sup> The total field at the receiver position is expressed as the sum of three components, two of them being the geometrical ones, the direct wave and the wave reflected on either or both of the wedge faces, and the wave diffracted by the wedge. There is no consideration in this work of the phenomenon of wave transmission through the wedge. Figure 1 illustrates the geometry of the problem with the faces of the wedge having the impedances  $Z_0$  and  $Z_n$  and being at the angles  $0$  and  $n\pi$  in the fluid medium ( $n$  is equal to 2 for a half plane), where:

$$\sin \theta_{0,n} = \frac{Z_c}{Z_{0,n}}, \quad (1)$$

$\theta_{0,n}$  being the Brewster angles of the wedge faces and  $Z_c$  the impedance of air, i.e.  $Z_c = \rho c$ ,  $\rho$  being the density of air, and  $c$  the speed of sound propagation. The incident wave is assumed being  $e^{-ikr} / \sqrt{kr}$ ,  $k$  being the wavenumber, and a time dependence factor  $e^{i\omega t}$  is understood and omitted throughout. The distance of the sound source to the edge of the wedge is  $r'$  and that of the field point is  $r$ . The corresponding angles made with the wedge face nearer to the sound source are respectively  $\varphi'$  and  $\varphi$ . The field diffracted by the wedge  $u^d$  may be written as the sum of four terms, that is  $u^d = \sum_{l,m=1}^2 u_{l,m}^d$  with:<sup>16</sup>

$$u_{l,m}^d = \frac{e^{-ikr}}{\sqrt{kr}} P_{l,m}(\varphi, \varphi') F \left[ k \frac{rr'}{r+r'} a_{l,m} \right] \frac{e^{-ikr}}{\sqrt{kr}}. \quad (2)$$

Note that this expression is the result of a high frequency asymptotic formulation. Hence, it is expected to be valid for frequencies down to a value such that the wavelength does not exceed a typical size in the problem, or equivalently that the location of either source or receiver be in the far field.

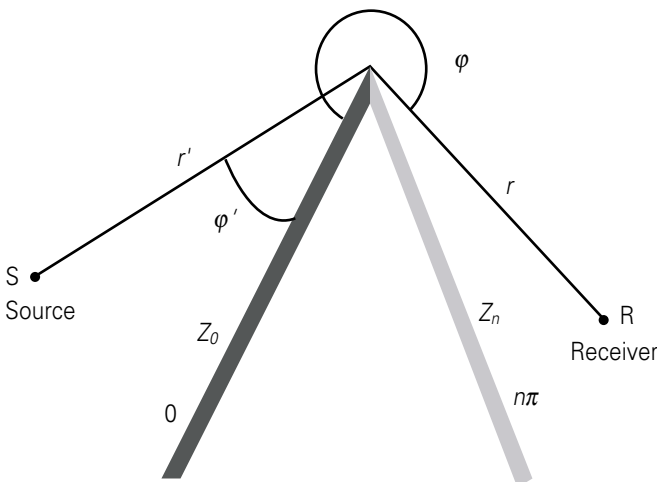


Fig. 1— Geometry of the problem of diffraction of an acoustical wave by an impedance wedge.

Furthermore, the present solution is uniform and is in full agreement with the expression formulated by the Uniform Theory of Diffraction (UTD) for the hard wedge, where the term  $P_{l,m}$  is given by :

$$P_{l,m}(\varphi, \varphi') = -\frac{e^{-i\pi/4}}{2n\sqrt{2\pi}} \Omega_n(\varphi, \varphi') \cdot (-1)^{l+m+1} A_n [(-1)^l \varphi, (-1)^m \varphi'] \cot \frac{\pi + (-1)^l \varphi + (-1)^m \varphi'}{2n} \quad (3)$$

where:

$$\Omega_n(\varphi, \varphi') = \frac{\psi_n^8(\pi/2)}{4\Psi(n\pi/2 - \varphi)\Psi(n\pi/2 - \varphi')} \quad (4)$$

and:<sup>13</sup>

$$A_n[\alpha, \alpha'] = \left[ \cos\left(\frac{\pi - 2\theta_0}{2n}\right) \cos\left(\frac{\pi - 2\theta_n}{2n}\right) - \cos^2\left(\frac{\pi}{2n}\right) \right] - \sin\left(\frac{\alpha}{n}\right) \sin\left(\frac{\alpha'}{n}\right) - \frac{1}{2\sin\left(\frac{\pi}{2n}\right)} \left[ \sin\left(\frac{\alpha}{n}\right) + \sin\left(\frac{\alpha'}{n}\right) \right] \cdot \left[ \cos\left(\frac{\pi - 2\theta_0}{2n}\right) - \cos\left(\frac{\pi - 2\theta_n}{2n}\right) \right]. \quad (5)$$

The function  $\Psi$  is the auxiliary function defined by:

$$\Psi(n\pi/2 - \eta) = \psi_n^4(\pi/2) \frac{\sin\left(\frac{\eta + \theta_0}{2n}\right) \sin\left(\frac{n\pi - \eta + \theta_n}{2n}\right)}{M_n(\eta)} \quad (6)$$

in which:

$$M_n(\eta) = \frac{\psi_n(n\pi - \eta - \pi/2 - \theta_0) \psi_n(\eta - \pi/2 - \theta_n)}{\psi_n(n\pi - \eta - \pi/2 + \theta_0) \psi_n(\eta - \pi/2 + \theta_n)} \quad (7)$$

and the function  $\psi_n(z)$  is the special function introduced by Maliuzhinets, and defined by:

$$\psi_n(z) = \exp \left[ -\frac{j}{8n} \int_0^z \int_{-j\infty}^{j\infty} \tan \frac{\pi v}{4n \cos(v - \mu)} dv d\mu \right]. \quad (8)$$

The function  $\psi_n(z)$  satisfies the parity relation  $\psi_n(-z) = \psi_n(z)$ , and the property for complex conjugate argument  $\psi_n(z^*) = \psi_n^*(z)$ . A simpler alternative definition of  $\psi_n(z)$  using a single integration is:<sup>19</sup>

$$\psi_n(z) = \exp \left[ -\frac{1}{2} \int_0^{\infty} \frac{\cosh(\mu z) - 1}{\mu \cosh\left(\frac{\pi}{2} \mu\right) \sinh(2nz)} d\mu \right] \quad (9)$$

and useful and accurate polynomial approximations to this function may also be found.<sup>20</sup> In Eq. (2) the factor  $F \left[ k \frac{rr'}{r+r'} a_{l,m} \right]$  is the transition function defined by Kouyoumjian and Pathak and expressed by:<sup>21</sup>

$$F(X) = 2j\sqrt{X} e^{jX} \int_{\sqrt{X}}^{\infty} e^{-j\tau^2} d\tau \quad (10)$$

with:

$$a_{l,m}(\gamma) = 2 \cos^2 \left( \frac{2n\pi N^\pm - \gamma}{2} \right) \quad (11)$$

$\gamma = \varphi + (-1)^l \varphi'$  and  $N^\pm$  the nearest integer satisfying the equality  $2n\pi N^\pm - \gamma = (-1)^l \pi$ .

### 3. REFLECTION OF A SOUND WAVE AT AN IMPEDANCE BOUNDARY

Usually, the total field  $u_{tot}$  above an impedance boundary may be expressed by  $u_{tot} = u_i + Qu_r$  where  $u_i$  is the direct field source-receiver and  $u_r$  the field from the image source as though the boundary were ideally hard and  $Q$  a factor taking into account the boundary's impedance.

#### A. Spherical wave incidence

##### 1. Boundary with a homogeneous impedance: Thomasson's model

According to this model, the total field at the receiver is made up of three contributions: a direct wave with the distance range  $R_1$ , a reflected wave with  $R_2$  as if the ground were perfectly hard, and a correction term taking into account the complex and finite impedance of the ground,<sup>22</sup> (see Fig. 2):

$$u_{tot} = \frac{e^{ikR_1}}{4\pi R_1} + \frac{e^{ikR_2}}{4\pi R_2} - \Psi_R \quad (12)$$

Let  $\beta$  be the specific point admittance of the boundary, i.e.  $\beta = \rho c / Z_c$ , with  $\rho$  the density of air, then:

$$\Psi_R = \begin{cases} \Psi_{SD} + \Psi_B & \text{Re}(\gamma_0) > 1 \text{ and } \text{Im}(\beta) < 0 \\ \Psi_{SD} & \text{else} \end{cases}, \quad (13)$$

$$\Psi_{SD} = \frac{k\beta}{2\pi} e^{ikR_2} \int_0^\infty \frac{e^{-kR_2 t}}{\sqrt{W_1}} dt, \quad (14)$$

$$W_1 = [\cos \alpha_0 + \beta]^2 + 2it[1 + \beta \cos \alpha_0] - t^2, \quad (15)$$

$$\text{Re}(\sqrt{W_1}) = \begin{cases} < 0 & \text{Re}(\gamma_0) > 1 \text{ Im}(\beta) < 0 \quad t > t_1 \\ > 0 & \text{else} \end{cases}, \quad (16)$$

$$t_1 = -\text{Im}(\beta) \frac{\text{Re}(\beta) + \cos \alpha_0}{1 + \cos \alpha_0 \text{Re}(\beta)}, \quad (17)$$

$$\Psi_B = \frac{1}{2} k\beta H_0^{(1)} \left[ k(x_S + x_R) \sqrt{1 - \beta^2} \right] e^{-ik(y_S + y_R)\beta}, \text{ and } \quad (18)$$

$$\gamma_0 = -\beta \cos \alpha_0 + \sqrt{1 - \beta^2} \sin \alpha_0, \text{ Re}[\sqrt{1 - \beta^2}] > 0. \quad (19)$$

The origin of the system of coordinates is assumed to be on the impedance ground between the source and receiver positions, and hence R and S have for coordinates  $S(-x_S, y_S, z_S)$  and  $R(x_R, y_R, z_R)$  (Fig. 2). The angle  $\alpha_0$  is the angle made by the incident ray at reflection on the boundary and the normal at the specular point of reflection, i.e.  $\cos \alpha_0 = (y_S + y_R) / R_2$ . The term  $\Psi_B$  as given in Eq. (18) may be considered as the expression of a surface wave contribution.

##### 2. Boundary with an impedance discontinuity: deJong et al.'s model

This model is semi-empirical and permits evaluation of the acoustical field above a flat boundary with an impedance discontinuity, Fig. 3. The source-receiver line is supposed to

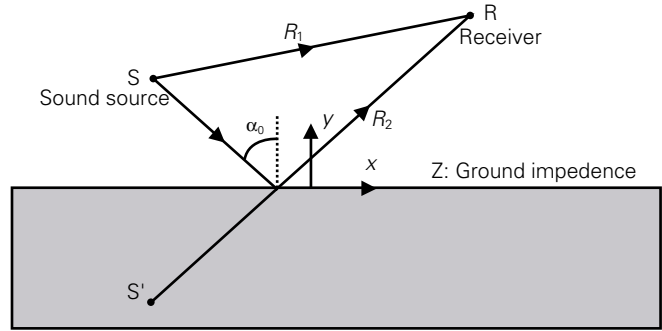


Fig. 2— Propagation of a spherical wave above an impedance boundary.

be normal to the impedance discontinuity line. For not too extreme geometrical situations and if  $u_i$  is the free field source-receiver, the excess attenuation due to the introduction of the

$$\frac{u}{u_i} = 1 + \frac{R_1}{R_2} Q_{1,2} e^{ik(R_2 - R_1)} + \frac{R_1}{R_3} (Q_2 - Q_1) \frac{e^{-i\pi/4}}{\sqrt{\pi}} \left\{ F[\sqrt{k(R_3 - R_1)}] \pm F[\sqrt{k(R_3 - R_2)}] e^{ik(R_2 - R_1)} \right\}, \quad (20)$$

$R_3$  being the two-segment distance source-receiver via the point of impedance discontinuity.  $Q_{1,2}$  are the wave reflection coefficients for an infinite boundary,  $F(x)$  is the Fresnel integral defined by:

$$F(x) = \int_x^{\infty} e^{iw^2} dw, \quad (21)$$

and  $Q_1$  ( $Q_2$ ) with + (-) is used in case the point of specular reflection falls on the boundary nearer (farther) from the sound source.<sup>4</sup> The purpose of introducing this model is to perform calculations on the efficiency of a barrier above a ground with different impedances on either side of the barrier. It is thus necessary to calculate the total sound field prior to erecting the barrier, and to compare its numerical performance to that of Manara et al.'s two-dimensional one. This is done at the end of the paper.

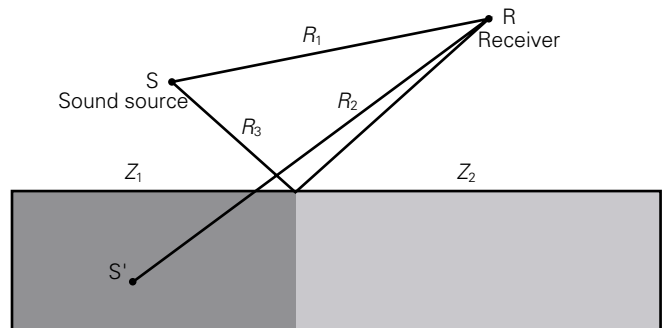


Fig. 3— Propagation of a spherical wave above a boundary with an impedance discontinuity.

## B. Cylindrical wave incidence

### 1. Boundary with a homogeneous impedance: Chandler-Wilde model

For a line source emitting a wave  $H_0^{(1)}(kR_1)$ , the total field above the impedance surface may be expressed as  $H_0^{(1)}(kR_1) + H_0^{(1)}(kR_2) + P_\beta$ ,  $P_\beta = P_\beta^{(l)} + P_\beta^{(s)}$  with:<sup>23</sup>

$$P_\beta^{(l)} = -\frac{4i\beta e^{ikR_2}}{\pi} \int_0^{+\infty} t^{-1/2} e^{-t} \frac{(\beta + \gamma(1+it))}{\sqrt{t - 2i(t^2 - 2i(1 + \beta\gamma)t - (\beta + \gamma)^2)}} dt \quad (22)$$

and:

$$P_\beta^{(s)} = \begin{cases} \frac{4i\beta}{\sqrt{1-\beta^2}} e^{ikR_2(1-a_*)}, & \text{Im } \beta < 0, \text{Re } a_* < 0 \\ \frac{4i\beta}{2\sqrt{1-\beta^2}} e^{ikR_2(1-a_*)}, & \text{Im } \beta < 0, \text{Re } a_* = 0 \\ 0, & \text{otherwise} \end{cases} \quad (23)$$

$a_* = 1 + \beta\gamma + \sqrt{(1-\beta^2) \cdot (1-\gamma^2)}$ , in which  $\beta = \rho c/Z$  is, as earlier, the normalized admittance of the surface and  $\gamma = (y_s + y_R)/R_2$ ,  $y_s$  and  $y_R$  being the heights of respectively the sound source and the receiver above the impedance plane. This model is introduced here for later use when the insertion loss of a barrier on the ground is considered. The usual approach for this kind of calculation is that the total field at the receiver located behind the barrier, evaluated using the classical ray technique, is made up of four contributions, all being diffracted at the top of the barrier, and their different combinations result from considering their reflections on either side of the barrier.

### 2. Boundary with an impedance discontinuity

The two-dimensional problem of sound propagation over an inhomogeneous ground is often solved by numerical techniques with appeal made to methods like Boundary Integral Equations. An overview on the use of such methods may be found in Chandler-Wilde and Hothersall's paper.<sup>24</sup> In this paper, however, the total field is expressed as the sum of the direct field, the reflected field on the impedance ground (taking the reflection coefficient of the nearest impedance side as in deJong's model). For the diffracted wave use is made of the theory for the wedge with different face impedances considering the wedge angle to be equal to  $180^\circ$ . As in section 3.A.2, in order for the efficiency of a barrier to be evaluated, the sound field above a two-impedance boundary needs to be calculated for a line source.

## 4. NUMERICAL EXAMPLES

### A. Edge diffraction by a finite impedance wedge in free space

The sound source being assumed linear, the field diffracted by the edge of the impedance wedge is calculated using Eqs (1-11). The results are presented in the surface plot of Fig. 4 where the amplitude of the edge diffracted field is expressed

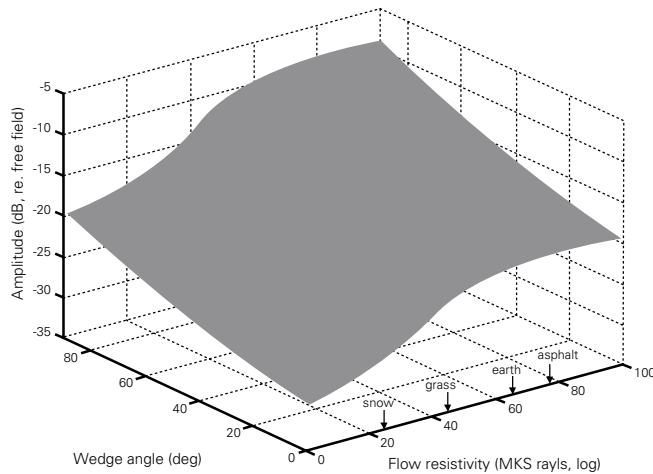


Fig. 4— Amplitude of the edge diffracted field as a function of flow resistivity and wedge angle.

as a function of the wedge angle and the flow resistivity.

The faces of the wedge have equal impedances, and are evaluated according to Delany-Bazley's model<sup>25</sup> with the resistivities as measured by Embleton et al.<sup>26</sup> For grass, the value of the flow resistivity was taken as  $\sigma_{\text{grass}} = 2.0 \times 10^5$  MKS rayls whereas for earth it was  $\sigma_{\text{earth}} = 6.0 \times 10^5$  MKS rayls. Although Delany-Bazley's model is known to have a limited range of validity, and that other more elaborate models (several parameter models) can definitely achieve superior performance, see for instance Attenborough's paper,<sup>27</sup> it is still the subject of improvements<sup>28</sup> and is being used as an acceptable approximation. The surface plot in Fig. 4 shows that the amplitude of the edge diffracted field increases with increasing impedance, and with increasing wedge angle. Note also the relatively strong variation of the field amplitude at low resistivity values and the slower rate of variation beginning from a value of the impedance resistivity corresponding approximately to that of grass.

Figure 5 shows the variation of the amplitude of the edge diffracted field with the wedge angle and for different frequencies. The larger the wavelength or the wedge angle, the larger is the amplitude of the edge diffracted field.

### B. Case of a finite impedance wedge barrier on ground with an impedance discontinuity

The effectiveness of a noise barrier is evaluated in terms of its insertion loss, IL, which is defined as the difference in dB of the sound pressure level at the receiver before,  $SPL_{\text{before}}$ , and after mounting the barrier on the ground,  $SPL_{\text{after}}$ .

$$IL = SPL_{\text{before}} - SPL_{\text{after}} \quad (24)$$

For the case of ground without a barrier, the total acoustical field at the receiver has been calculated according to the method described in section 3.B.2, that is the field is evaluated as though the angle of the wedge with different face impedances is equal to  $180^\circ$ . Figure 6 illustrates the frequency variation of the sound pressure level for two kinds of wedge

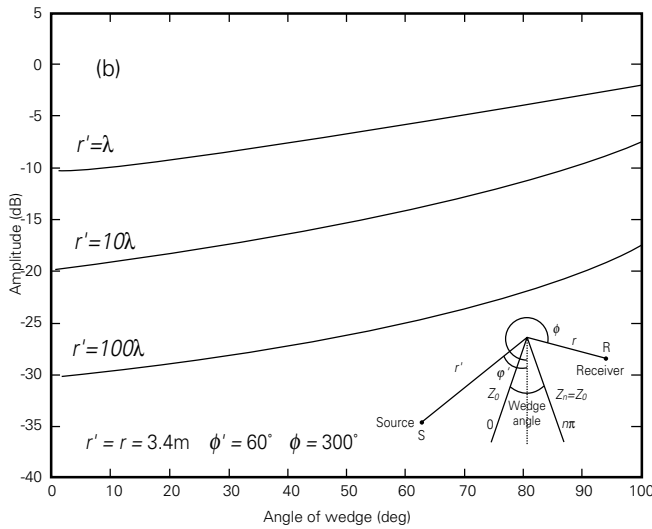
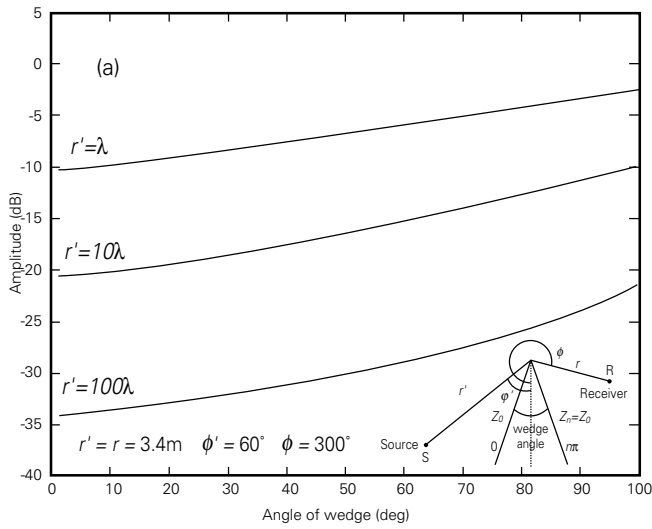


Fig. 5— Amplitude of the edge diffracted field vs. wedge angle and frequency. a) grass wedge with  $\sigma_{grass} = 2.0 \times 10^5$  MKS rayls, and b) earth wedge with  $\sigma_{earth} = 5.0 \times 10^5$  MKS rayls.

barriers, a soft one made of grass, and a hard one made of earth, on a ground that is asphalt-like on the source side and grass-like on the receiver side. The values of the flow resistivities for grass and earth were taken as previously while for asphalt  $\sigma_{asphalt} = 3.0 \times 10^7$  MKS rayls. The total pressure field at the receiver may be considered as the sum of four components represented by the wave propagation paths from the sound source, or its image through the ground, to the receiver, or its image through the ground, via the top of barrier. It may also be noted from the spectra of sound pressure that there is a lesser effect of the wedge angle on the insertion loss for the softer barrier towards higher frequencies, whereas the effect of the wedge angle is about of the same order for both barriers in the low frequency range. Figure 7 shows the insertion loss (IL) as a function of the barrier angle, and in both cases of the barrier, the IL is found to decrease with increasing wedge angle. With reference to Fig. 6, the data were considered as S(-10m,

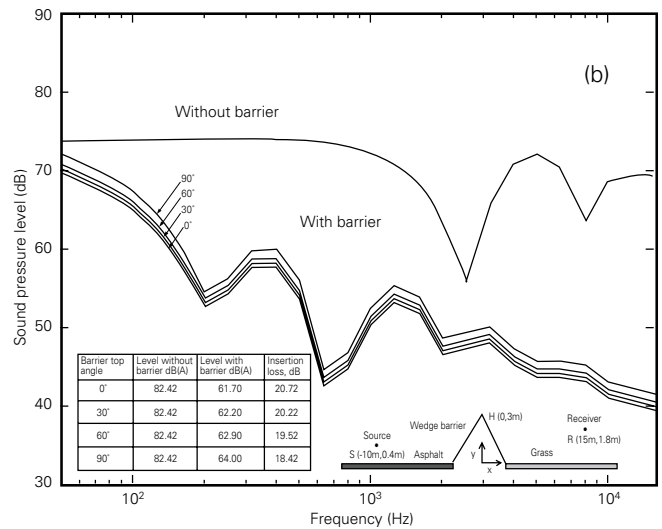
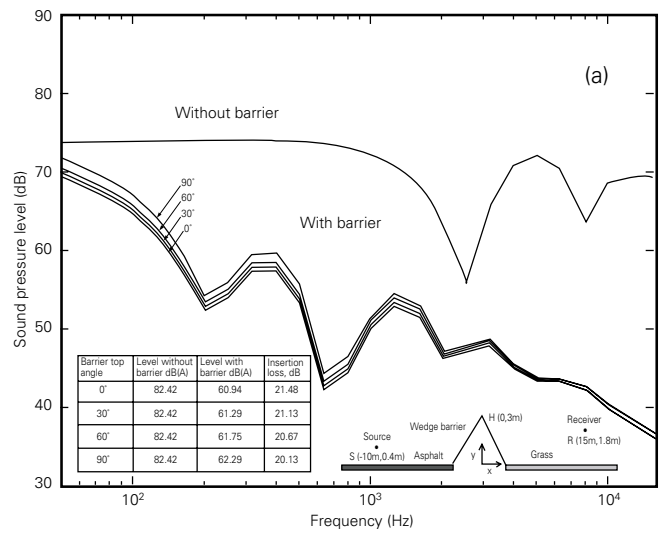


Fig. 6— Spectra of sound pressure level of a wedge barrier on an asphalt-grass ground with  $\sigma_{asphalt} = 3.0 \times 10^7$  MKS rayls. a) grass wedge barrier,  $\sigma_{grass} = 2.0 \times 10^5$ , and b) earth wedge barrier,  $\sigma_{earth} = 5.0 \times 10^5$  MKS rayls.

0.4m), R(15m, 1.8m) and H(0, 3.0m). It is also of interest to note the greater sensitivity of the harder barrier towards larger values of its angle. Moreover, the calculations show that the earth barrier accomplishes a performance about 1 dB to 2 dB less than that of the grass barrier. With reference to Fig. 5, it is thus possible to generalize that in terms of noise reduction a barrier has a better performance the thinner and the softer it is.

Lastly, a comparison is made between calculating the IL for a line, and for a point-like sound source (see Fig. 8). The performance of the barrier, ideally hard in this case, is to some extent better when a spherical source is considered. The IL is also found to follow a monotonous variation with the wedge angle, though with a somehow stronger decrease for larger wedge angles. These observations are in agreement with the results of previous studies where the two-

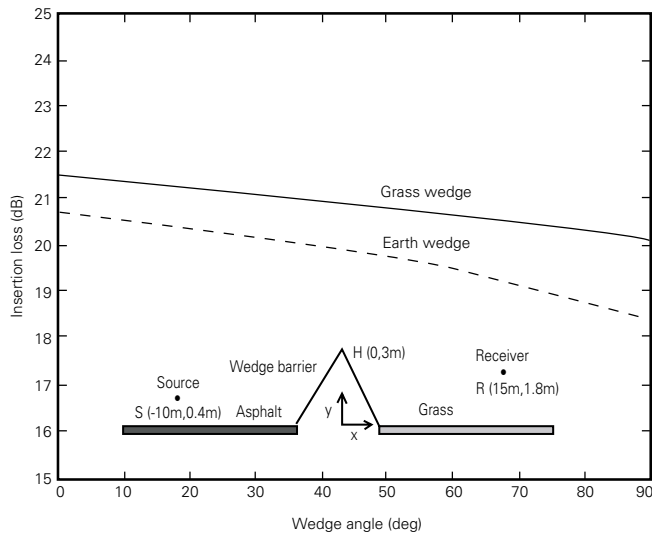


Fig. 7— Insertion loss of a wedge barrier vs. wedge angle. a) grass wedge,  $\sigma_{grass} = 2.0 \times 10^5$  MKS rayls. b) earth wedge,  $\sigma_{earth} = 5.0 \times 10^5$  MKS rayls.

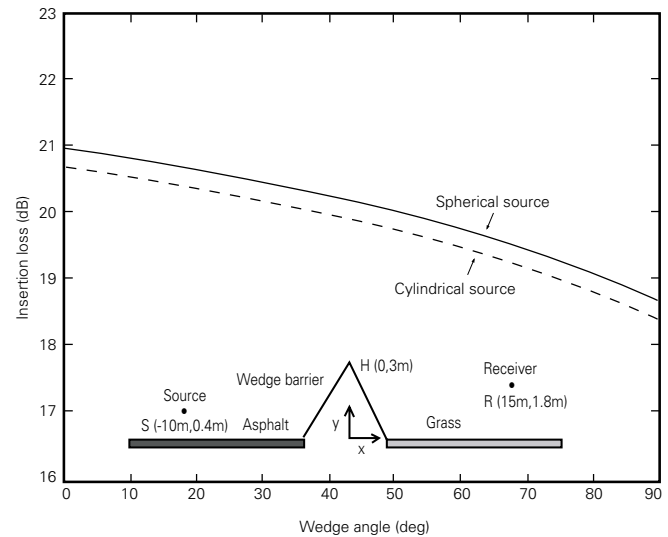


Fig. 8— Insertion loss of a hard wedge barrier vs. wedge angle for different sound sources.

dimensional formulation was numerically solved using the BEM method.<sup>29</sup>

## 5. CONCLUSIONS

This study was concerned with the problem of sound attenuation by an absorbing wedge shaped barrier on finite impedance ground. The model used in the numerical calculations is for a line source excitation. The edge diffracted field is given in an explicit form as a high frequency asymptotic expression resulting from the adoption of an exact solution to the case of plane wave incidence. The model is of more general application as the wedge barrier may be considered as having different boundary conditions on its faces. The present study however focused on a wedge with equal face impedances. The results of numerical computations show that the amplitude of the edge diffracted field increases for increasing wedge angle. Furthermore, the amplitude of this field also increases for increasing flow resistivity of the wedge impedance, and the harder the wedge-like barrier, the lower its sound shielding effectiveness. Hence, the performance of an absorbing wedge barrier decreases for increasing top angle and for increasing impedance. Similar conclusions can also be drawn for a hard wedged barrier and with a point-like sound source. The examples treated in this study may serve as guidance for the design of noise barriers, which to increase effectiveness are required to be as thin and as soft as possible.

An improvement in the numerical predictions presented in this work may be achieved by considering multiple diffraction between the top and the base of the barrier. Indeed, for instance the wave diffracted at the top of the barrier may propagate along one of the faces of the barrier then to be diffracted at the base line connecting the barrier to the ground.

## 6. REFERENCES

- G. D. Maliuzhinets, "Excitation, reflection and emission of surface waves from a wedge with given face impedances," *Soviet Physics Doklady* **3**, 752-755 (1958).
- H. G. Jonasson, "Diffraction by wedges of finite acoustic impedance with applications to depressed roads," *J. Sound Vib.* **25**, 577-585 (1972).
- A. D. Pierce and W. J. Hadden, "Diffraction of a plane wave by a wedge with finite impedance," *J. Acoust. Soc. Am.* **63**, 17-27 (1978).
- B. A. DeJong, A. Moerkerken, and J. D. Van Der Toorn, "Propagation of sound over grassland and over an earth barrier," *J. Sound Vib.* **86**, 23-46 (1983).
- S. I. Hayek, "Acoustic diffraction by absorbent wedge-shaped barriers," *Proc. INTER-NOISE 84*, edited by George C. Maling, Jr. (Noise Control Foundation, Poughkeepsie, New York, 1984), Vol. 1, pp. 313-318.
- A. M. J. Davis, "Two-dimensional acoustical diffraction by a penetrable wedge," *J. Acoust. Soc. Am.* **100**, 1316-1324 (1996).
- W. T. Hadden and A. D. Pierce "Sound diffraction around screens and wedges for arbitrary point source locations," *J. Acoust. Soc. Am.* **69**, 1266-1276 (1981).
- J. S. Robertson, "Sound propagation over a large wedge: a comparison between the geometrical theory of diffraction and the parabolic equation," *J. Acoust. Soc. Am.* **106**, 113-119 (1999).
- P. Menounou, I. J. Busch-Vishniac, and D. T. Blackstock, "Directive line source: a new model for sound diffraction by half planes and wedges," *J. Acoust. Soc. Am.* **107**, 2973-2986 (2000).
- D. I. Butorin and P. Y. Ufimtsev, "Explicit expression for an acoustic edge wave scattered by an infinitesimal edge element," *Sov. Phys. Acoust.* **32**, 283-287 (1987).
- D. Chu, "Impulse response of density contrast using normal coordinates," *J. Acoust. Soc. Am.* **86**, 1883-1896 (1989).
- H. H. Syed, "PTD analysis of impedance structures," *IEEE Trans. Ant. Prop.* **AP-44**, 983-988 (1996).
- R. Tiberio, G. Pelosi, and G. Manara, "A uniform GTD formulation for the diffraction by a wedge with impedance faces," *IEEE Trans. Ant. Prop.* **AP-33**, 867-872 (1985).
- R. G. Rojas, "Electromagnetic diffraction by a wedge with impedance faces," *IEEE Trans. Antenn. Prop.* **AP-36**, 956-970 (1988).
- T. Griesser and C. A. Balanis, "Reflections, diffractions, and surface waves for an interior impedance wedge of arbitrary angle," *IEEE Trans. Antenn. Prop.* **AP-37**, 927-935 (1989).

- <sup>16</sup> G. Manara, R. Tiberio, G. Pelosi, and P. H. Pathak, "High frequency scattering from a wedge with impedance faces illuminated by a line source, part I: diffraction," *IEEE Trans. Antenn. Prop.* **AP-41**, 212-218 (1993).
- <sup>17</sup> G. Manara, R. Tiberio, G. Pelosi, and P. H. Pathak, "High frequency scattering from a wedge with impedance faces illuminated by a line source, part II: surface waves," *IEEE Trans. Antenn. Prop.* **AP-41**, 877-883 (1993).
- <sup>18</sup> J. F. Rouviere, N. Douchin, and P. F. Combes, "Diffraction by lossy dielectric wedges using both heuristic UTD formulations and FDTD," *IEEE Trans. Antenn. Prop.* **AP-47**, 1702-1708 (1999).
- <sup>19</sup> V. Zavadskii and M. Sakharova, "Application of the special function in problems of wave diffraction in wedge-shaped regions," *Sov. Phys. Acoust.* **13**, 48-54 (1967).
- <sup>20</sup> M. I. Herman, J. L. Volakis, and T. B. A. Senior, "Analytic expressions for a function occurring in diffraction theory," *IEEE Trans. Antenn. Prop.* **AP-35**, 1083-1086 (1987).
- <sup>21</sup> R. G. Kouyoumjian and P. H. Pathak, "A uniform asymptotic theory of diffraction for an edge in a perfectly conducting surface," *Proc. I.E.E.E.* **62**, 1448-1461 (1974).
- <sup>22</sup> S. I. Thomasson, "Reflection of waves from a point source by an impedance boundary," *J. Acoust. Soc. Am.* **59**, 780-785 (1976).
- <sup>23</sup> S. N. Chandler-Wilde and D.C. Hothersall, "Efficient calculation of the Green function for acoustic propagation above a homogeneous impedance plane," *J. Sound Vib.* **180**, 705-724 (1995).
- <sup>24</sup> S. N. Chandler-Wilde and D.C. Hothersall, "Sound propagation above an inhomogeneous impedance plane," *J. Sound Vib.* **98**, 475-491 (1985).
- <sup>25</sup> M. E. Delany and E. N. Bazley, "Acoustical properties of fibrous absorbent materials," *Appl. Acoust.* **3**, 105-116 (1970).
- <sup>26</sup> T. F. W. Embleton, J. E. Piercy, and G. A. Daigle "Effective resistivity of ground surfaces determined by acoustical measurements," *J. Acoust. Soc. Am.* **74**, 1239-1244 (1983).
- <sup>27</sup> K. Attenborough, "Acoustical impedance models for outdoor ground surfaces," *J. Sound Vib.* **99**, 521-544 (1985).
- <sup>28</sup> M. Yasushi, "Acoustical properties of porous materials-modifications of Delany-Bazley Models," *J. Acoust. Soc. Jap. (E)* **11**, 19-24 (1990).
- <sup>29</sup> A. Muradali and K. R. Fyfe, "A Study of 2D and 3D barrier insertion loss using improved diffraction-based methods," *Appl. Acoust.* **53**, 49-75 (1998).